



E-scooter Vibration Impact on Driver Comfort and Health

Juan D. Cano-Moreno¹ · Manuel E. Islán¹ · Fernando Blaya¹ · Roberto D'Amato¹ · Juan A. Juanes² · Enrique Soriano³

Received: 22 September 2020 / Revised: 4 January 2021 / Accepted: 6 January 2021
© Krishtel eMaging Solutions Private Limited 2021

Abstract

Background Micro-mobility provides a solution for last mile problem and e-scooter sharing systems are one of the most heavily adopted micro-mobility services. The increasing usages of e-scooters make it necessary to analyze the possible effects of the vibrations transmitted to the drivers.

Purpose This research has studied for the first time the e-scooter vibrations effects on drivers comfort and health for the actual range of circulation speeds, that can exceed 25 km/h.

Methods Based on experimental measured stiffness of two different e-scooter wheels and Multibody dynamic simulations, several statistical models have been obtained following the standard UNE2631.

Results The results show that for a common e-scooter and a road profile with a very good-good roughness level, a velocity of 16 km/h starts to be uncomfortable and for 23 km/h could be harmful for health, for short trip durations. Derived from the statistical models, a new way of measuring the roughness has been proposed and that will be one of the future works to adjust and validate it.

Conclusion E-scooter suspension systems (front suspension and wheels) must be improved under human comfort and health point of view. Furthermore, results suggest the necessity of study the vibrations effects on real e-scooters due to the maximum speed they can reach is greater than 25 km/h.

Keywords Ride comfort · E-scooter · Road profile · Multibody dynamics · Urban transport

Introduction

Climate change consequences have created a social awareness about the need of acquiring sustainable lifestyle habits. However, since globally, the population trends to become urban, the cities and their citizens must lead the fight to face climate change challenges.

In the cities, transport plays a crucial role in the urban development and in the citizens daily habits and it is the second largest sector contributing to global emission from

fossil fuel combustions, so sustainable transport is a commitment to accelerate the transition to sustainable development.

Under the umbrella of the implementation methods for sustainable urban transport in a city, it is increasingly common to see alternative electric transports. In the fact, the sales of new electric vehicles have increased in near 800% in the last 5 years [1] But it is in the last mile transportation in which the electric vehicles have revolutionized the citizen's transportation habits.

Last mile concept come from telecommunications industry to describe the difficulty of connecting end user's homes and businesses to the main telecommunication network. Now, this concept [2] is used also for both transporting people and freight [3]. For people, last mile describe the difficulty in getting people from transportation hubs (railway station, bus depots, ferry berths, etc.) to their final destination and vice versa.

In this sense, in the last 5 years, the last mile transportation has expansion towards electric based vehicles, with many different solutions, including feeder buses, bicycle

✉ Juan D. Cano-Moreno
juandavid.cano@upm.es

¹ E.T.S. de Ingeniería Y Diseño Industrial, Universidad Politécnica de Madrid, Madrid, Spain

² Facultad de Medicina, University of Salamanca, Salamanca, Spain

³ Departamento de Ingeniería Mecánica, University of Carlos III of Madrid, Madrid, Spain

sharing systems [4], car sharing [5], personal rapid transit cars (pod cars) [6] and motorized shoes [7], and over all, the dockless electric scooters (e-scooters). The revolution of these electric transportation solutions has been accompanied by a new transportation concept, from vehicle ownership to vehicle sharing [8–10]. Gössling [11] shows an overview about e-scooters as one of the transport that will transform the automotive systems.

Starting in late 2017, and following the rapid development of mobile communication technology, micro-mobility services have entered the marketplace by sharing vehicles such as dockless electric scooters (e-scooters), this means that user can drop off and pick up from arbitrary locations, without a fixed home location. E-scooter sharing systems have a great international expansion. In Europe, from 2017 to 2018, the amount of shared e-scooters was increased by nearly 200% [12]. The European demand is expected to grow more than 25% per year until 2025. Other publications [13–17] also confirm the growing importance of the e-scooter in various parts of the world.

Micro-mobility provides a solution for last mile problem and e-scooter sharing systems are one of the most heavily adopted micro-mobility services, although there are some alternative means of transport [18]. The consolidation of e-scooter as a sustainable transport must be accompanied by safe, reliable and healthy transport consideration, but the rapid expansion of these vehicles has dismissed the potential health problems for their drivers, focusing in regulation aspects.

This paper presents a research focused on e-scooters impact on drivers comfort and health. As we argued, they are and will be more and more a part of the daily landscape [19] in urban environments.

E-scooters come from the child skate design, used as a toy, but they can reach higher velocities, exceeding 20 km/h. Not all e-scooters have an additional damping system to the wheels themselves, and some of them still have very rigid wheels. Their mechanical design and the growing usage of e-scooters make it necessary to analyze the possible effects

of the vibrations transmitted to the driver. There are several investigations about this topic for other means of transport [20–26].

The main objective of this paper is to quantitatively assess on the vibration's effects on comfort and health of the e-scooter driver based on the velocity and quality of the road on which it is traveling. This assessment will be carried out for different types of wheels and front suspension, developing statistical models for explaining the variability of both, the comfort and health indexes, with these parameters: velocity, road roughness, road–tire contact stiffness and the stiffness of the front suspension.

Materials and Methods

The research presented in this paper is based on the methodology developed by Cano-Moreno et al. [27]. This methodology will be applied to a specific e-scooter layout, varying the stiffness of the suspension elements and considering the road irregularities. This methodology included two main domains, simulation and postprocessing the simulation results. As Fig. 1 shows, in this paper, a design of experiment and a statistical analysis of results will be added to postprocessing domain.

The e-scooter model layout analyzed in this research is a two-wheel e-scooter with a wheelbase of 1083 mm and a height from the ground of 1194 mm. It has been assumed in this case that driver is standing because it is the most used layout in urban environments until now. Thus, the layout corresponds to that shown in Fig. 1, where the reference system to be used is shown, X axis for the longitudinal direction of advance and Z axis, vertical axis. This reference system is located just in the middle of two wheel centers.

Dynamic Model

A Multibody model has been developed for running dynamic simulations, based on the proposal of Cano-Moreno et al.



Fig. 1 Methodology scheme and e-scooter layout

[27]. This model has been implemented in Simscape, a Simulink library (in the Matlab 2018B version). For simulation, we have to define force elements, inertia and mass properties. The velocity and road profiles are also inputs of the model. The following sections justify the values to be used for both stiffness (k_w) and damping (d_w) of the wheel–road contact and the front suspension (k_{fs} and d_{fs}). Figure 2 shows the topologic diagram of the Simscape model. This model represents a 2D model, with three main bodies, two wheels (m_t) and a body for e-scooter frame (m_s) and driver body (m_d) as a rigid solid. A translational joint has been defined between the wheels to establish a most real compatibility in the Multibody behavior. This is because with the existence of a tilted front suspension the distance between the tire centers is not kept constant.

The main parameters are described in Table 1.

Model equations is going to be presented to better understand the force elements and joints in the topologic diagram presented in Fig. 2. First, the road excitation input will be explained.

The road profile input is simulated as an imposed displacement on two bodies respect to a fixed reference coordinate system. The displacements are introduced in the model through prismatic joints. These displacements are according to the roughness of the road and there are the excitations of the dynamic model. The excitation, named $Z_r(t)$, is the same for

Table 1 Dynamic model notation

Parameter	Meaning
m_s [kg]	E-scooter frame mass
m_d [kg]	Driver mass
m_t [kg]	Tire mass
k_w [N/m]	Wheel–road contact stiffness
k_{fs} [N/m]	Front suspension stiffness
d_w [Ns/m]	Wheel–road contact damping
d_{fs} [Ns/m]	Front suspension damping

both the bodies which are in contact with each tire. As a notation convention, it has been used “b” for back and “f” for front items following the selected forward direction, indicated in figure. Then, the displacement of two tires can be expressed as:

$$Z_{rf} = Z_r(t) \tag{1}$$

$$Z_{rb} = Z_r\left(t + \frac{w_d}{v}\right), \tag{2}$$

where w_d is the distance between tire centers and v is the constant selected velocity and t is the simulation time. The vertical coordinate of the main body at its center of mass,

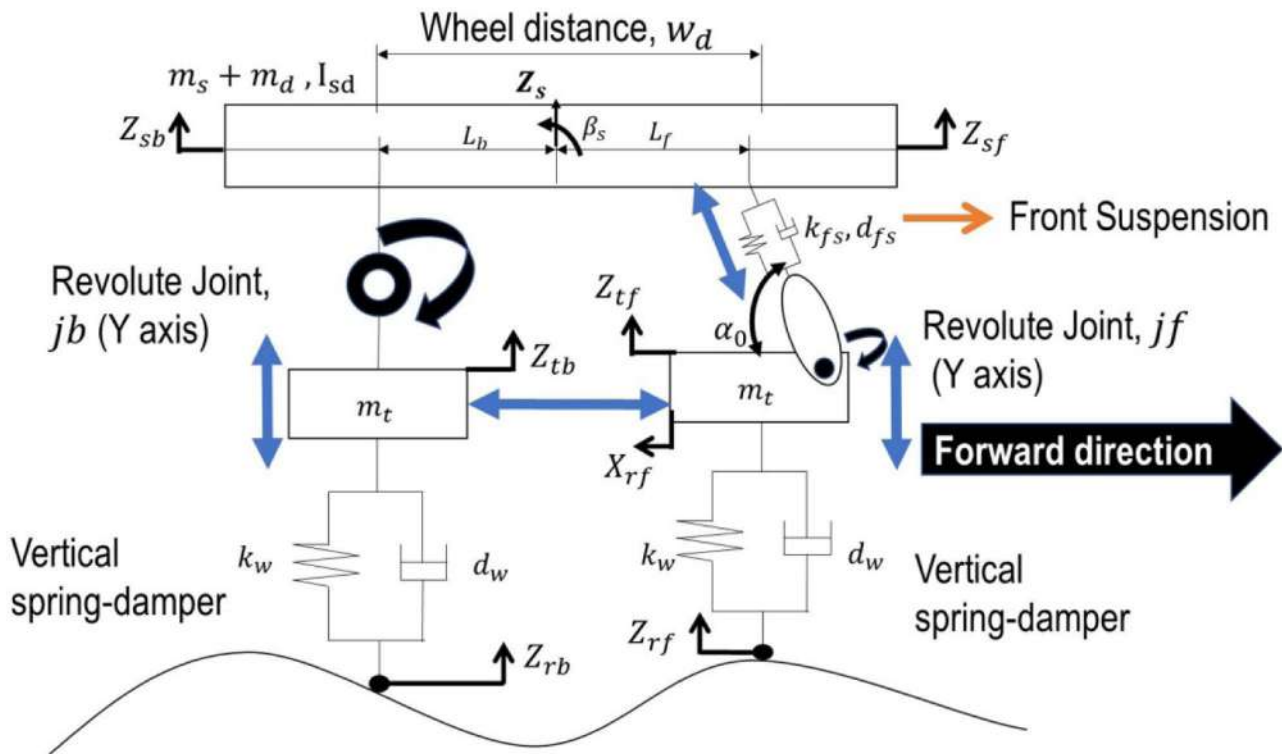


Fig. 2 Topologic diagram of dynamic model

can be expressed in function of the two vertical coordinates of the e-scooter extremes, situated in a symmetric way:

$$Z_s = \frac{Z_{sb} + Z_{sf}}{2}. \quad (3)$$

The equations of e-scooter suspension system of the proposed model are represented in Eqs. (4)–(10). The main body is composed of the e-scooter frame and the e-scooter driver body. The equation for the vertical motion at this main body can be represented as the following equation:

$$(m_s + m_d) \times \ddot{Z}_s + d_{fs} \times \cos(\alpha_0) \times (\dot{Z}_{sf} - \dot{Z}_{tf}) + k_{fs} \times \cos(\alpha_0) \times (Z_{sf} - Z_{tf}) - f_{z_{jb}} = 0, \quad (4)$$

where α_0 is the fixed angle between the front suspension system and a vertical line. Note that $f_{z_{jb}}$ is the vertical force for maintaining the revolute joint between the back tire and the e-scooter frame. The equations for the vertical motion of tires are

$$m_t \times (\ddot{Z}_{tb} - \ddot{Z}_{rb}) - d_w \times (\dot{Z}_{tb} - \dot{Z}_{rb}) - k_w \times (Z_{tb} - Z_{rb}) + f_{z_{jb}} = 0, \quad (5)$$

$$m_t \times (\ddot{Z}_{tf} - \ddot{Z}_{rf}) - d_w \times (\dot{Z}_{tf} - \dot{Z}_{rf}) - k_w \times (Z_{tf} - Z_{rf}) + f_{z_{jf}} = 0. \quad (6)$$

The force in the front revolute joint can be expressed in relation with the spring-damper force element of the front suspension system:

$$f_{z_{jf}} = k_{fs} \times \cos(\alpha_0) \times (Z_{sf} - Z_{tf}) + d_{fs} \times \cos(\alpha_0) \times (\dot{Z}_{sf} - \dot{Z}_{tf}), \quad (7)$$

$$f_{X_{jf}} = f_{z_{jf}} \times \tan(\alpha_0). \quad (8)$$

Both tires have a translational joint that allows their relative movement in longitudinal direction. For the longitudinal motion, Eq. (8) is presented as:

$$m_t \times \ddot{X}_{rf} - f_{X_{jf}} - f_{X_{jb}} = 0. \quad (9)$$

The equation of motion for the pitch moment of the main body can be presented as:

$$I_{sd} \times \ddot{\beta}_s + L_f \times [d_{fs} \times \cos(\alpha_0) \times (\dot{Z}_{sf} - \dot{Z}_{tf}) + k_{fs} \times \cos(\alpha_0) \times (Z_{sf} - Z_{tf})] - L_b \times [f_{z_{jb}}] = 0, \quad (10)$$

where I_{sd} is the inertial moment around the rotation axis, β_s is the rotation angle of this main body, L_b is inter-space between back axle and the main body center of gravity and L_f is inter-space between front suspension system anchorage and the main body center of gravity.

The mass and inertial properties of both the scooter and the person who drives it will also be calculated. Finally, it will be explained how the artificial random road profiles have been generated for different roughness values. Next

figure shows the Simscape (Simulink) block diagram used in this research (see Fig. 3).

Wheel–Road Contact

The wheels of the e-scooters can be made of different materials. Three main types have been found: pneumatic or rigid rubber wheels and polyurethane wheels. These materials assume different wheel–road contact stiffness, the pneumatic ones being the least rigid while those of polyurethane are

the most rigid.

The wheel–road contact is modeled as a force element of the spring-damper type. No publications have been found with this stiffness and damping values. Thus, an experiment has been carried out for two types of e-scooter tires: a small and rigid tire (13 cm outer diameter) and a pneumatic tire (25 cm of outer diameter) with inner air chamber. For compression tests, a model TN-MD machine (HOYTOM, S.L., Bilbao, Spain), motorized with automatic control was used. Its capacity is 200 kN, the piston stroke length is 125 mm, and the displacement rate was fixed at 0.5 mm/min. Experiments have been performed by establishing a maximum force of 2000 N. Results show the mean stiffness values for both tires. For pneumatic tire, the mean stiffness values vary from 0.9E5 to 1.3E5 N/m, depending the inflation pressure, 30 psi and 60 psi, respectively. Rigid tire mean stiffness reach the higher value, 3.6E5 N/m. Taking into account these tests, a range of tire–road contact stiffness from 0.5 to 4E5 N/m will be studied.

These values are consistent with others present in the literature. Thus, the values published by Agostinacchio et al. [28] show a stiffness of 1.5E5 N/m. Ramji et al. [29] published a series of stiffness curves for small tires based on load. For the minimum value of these curves, around 1 kN and maximum inflation pressure 262 kPa (38 psi) have vertical stiffness values of the order of 1.55E5 N/m.

The damping of the tires used in other investigations is usually low, even nil. Heißing and Ersoy [30] indicate that the damping value of a tire is almost negligible, that values of 50 Ns/m or 100 Ns/m can be used. Following this recommendation, the value of 100 Ns/m has been used for all simulations. Tire mass, m_t , has been considered 1 kg based on weights of commercial e-scooter tires (around 0.5–1.5 kg). They have been considered as punctual masses without inertial properties.

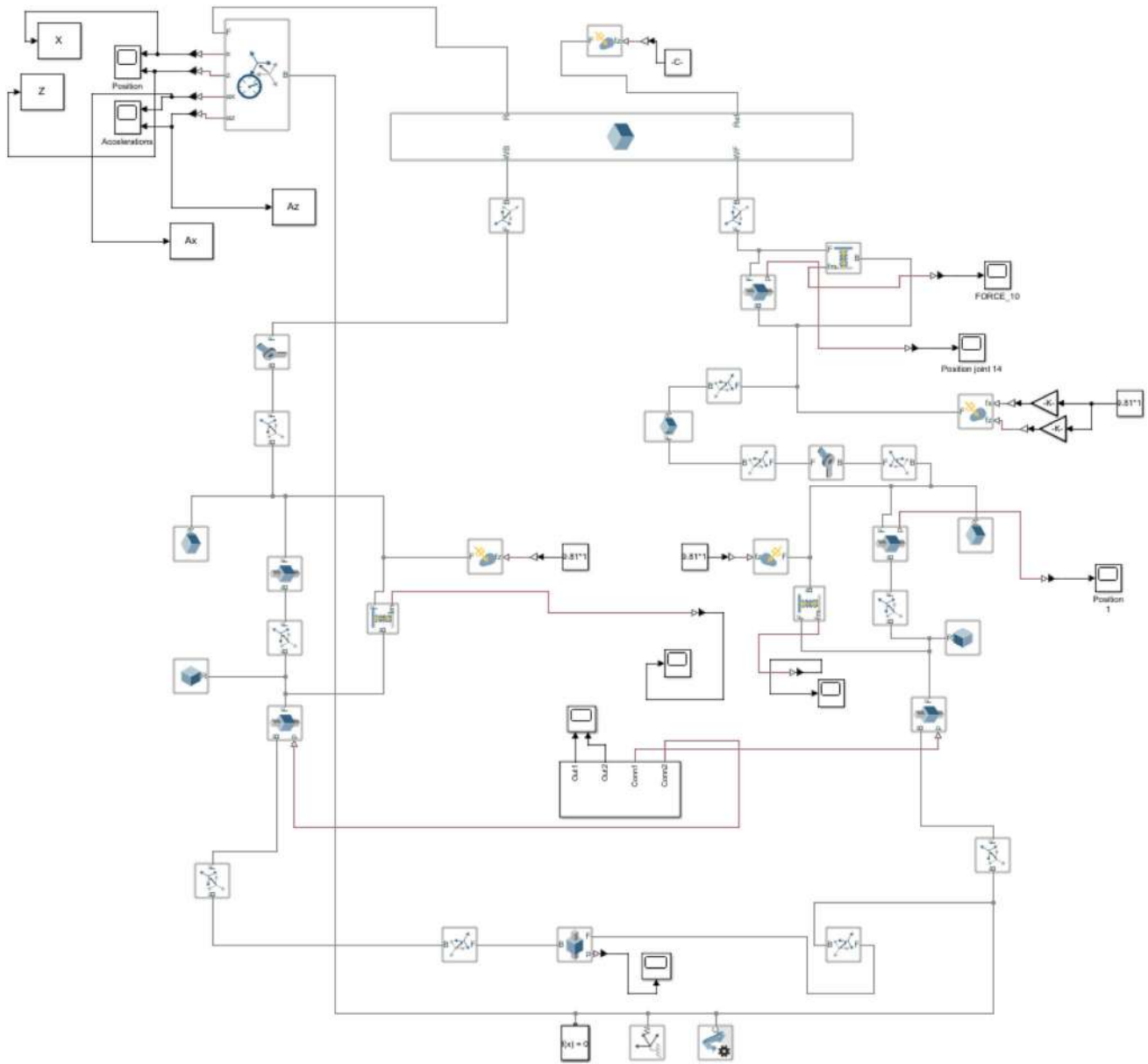


Fig. 3 Simscape (Simulink) block diagram

Front Suspension

For the spring of the front suspension are taken into account commercial values [18] that define most used range between 750 lb/in (1.3E5 N/m) and 2000 lb/in (3.5E5 N/m). For the calculation of the damping, a value of 25% of the critical damping, d_{fsc} , has been assumed, used by the other authors [31]. Therefore, you have the following value:

This research has focused on the study of the influence of the value of the stiffness of this suspension, so 3 stiffness values of this suspension will be studied in the design of experiments: 1.3E5 N/m, 2.4E5 N/m and 3.5E5 N/m. For a more rigid suspension, even without suspension system, a higher value of 1.E6 N/m has been also studied. Although there are other front suspension systems [32], these values and layout

$$d_{fs} \left[\frac{Ns}{m} \right] = \xi \times d_{fsc} = 0.25 \times \left[2 \times \sqrt{k_{fs} \times \left(\frac{m_s + m_d}{2} \right)} \right] = 0.5 \times \sqrt{k_{fs} \times \left(\frac{m_s + m_d}{2} \right)}. \tag{11}$$

covers most of models used by rental companies for solving last mile problem.

Inertia Propeties

Wheels have been assumed to be punctual masses, while the inertial properties of the e-scooter frame and the driver's body are included. First, the properties of the e-scooter frame are shown, not including the wheels. For this, a simplified e-scooter has been modeled including the base, the fork guide and the handlebar. It has been assumed as material, steel and all properties have been referred to axes that coincide with the area where the user steps (see Table 2).

The center of gravity with respect to the reference system [X, Z] is [150.7, 181.2] mm and it has a mass of 10.741 kg. Chandler et al. [33] and Santschi et al. [34] have published values for inertia parameters and center of gravity values for human body in different positions. To calculate the moments of inertia and center of gravity of the driver, average values proposed by Chandler et al. [33] have been used. In this research, the inertial properties are collected for the entire body standing, sitting and every member of the human body separately.

It is observed that the moments of inertia of the arm, forearm and hand are negligible compared to those of the whole

Table 3 Standing human inertia properties

Inertia properties	Values [33]	Values [34]	Simulation values
Center of gravity [%height]	41.43%	44.6%	43% (71.81 cm)
Mass [kg]	65	75.5	71
I_{xx} [kg × m ²]	11.9	11.6	11.7
I_{yy} [kg × m ²]	13.4	13	13
I_{zz} [kg × m ²]	1.7	1.3	1.5

body standing, so these values will be taken for simulations. The reference axis that will be used will be the following:

- Axis X, longitudinal, forward direction.
- Axis Z, vertical, positive upward.
- Axis Y, lateral, forming a right-handed system XYZ.

According to these axes, Table 3 shows the main moments of inertia of a human body standing, referring to its center of gravity. This table shows the values of two different authors and those selected for the simulation, which are intermediate values. A woman from Northern Europe, 71 kg and 1.67 m tall, has been selected [35].

The set of the user and the frame of the e-scooter will be assumed as a single rigid solid, so that the properties have been calculated from the properties of each one. For the center of gravity, in two dimensions, these values are found as:

$$Z_g = \frac{Z_{g_{user}} \times m_d + Z_{g_{frame}} \times m_s}{M + m} = \frac{0.7181 \times 71 + 0.1812 \times 10.741}{71 + 10.741} + 0.025 = 0.673 \text{ m}, \tag{12}$$

$$X_g = \frac{X_{g_{user}} \times m_d + X_{g_{frame}} \times m_s}{M + m} = \frac{0 \times 71 + 0.1507 \times 10.741}{71 + 10.741} = 0.02 \text{ m}. \tag{13}$$

The total mass of the rigid solid is 81,741 kg. The moments of inertia are the sum of the respective moments referenced to

Table 2 E-scooter frame inertia properties


	Inertia properties	
	I_{xx} [kg m ²]	1.588
	I_{yy} [kg m ²]	2.672
	I_{zz} [kg m ²]	1.133
	I_{xy} [kg m ²]	$2.518 \cdot 10^{-10}$
	I_{xz} [kg m ²]	-0.728
	I_{yz} [kg m ²]	$2.847 \cdot 10^{-10}$

Table 4 Standing human inertia properties

Inertia properties	E-scooter frame	Driver body	Sum
I_{xx} [kg × m ²]	1.588	50.906	52.494
I_{yy} [kg × m ²]	2.672	52.206	54.878
I_{zz} [kg × m ²]	1.133	1.5	2.633
I_{xy} [kg × m ²]	2.518×10^{-10}	0	2.518×10^{-10}
I_{xz} [kg × m ²]	-0.728	0	-0.728
I_{yz} [kg × m ²]	2.847×10^{-10}	0	2.847×10^{-10}

the same reference system. To obtain the user inertia values on the X and Y axis, it is necessary to apply the Steiner theorem, obtaining its values at the base of the scooter or the driver's feet. The Z axis matches. To use the same reference frame of the Multibody model, it is necessary to take into account that rigid reference frame is 25 mm higher than the other (Z direction):

$$I_{xx} = I_{xx}(CoG) + m_d \times Z_g^2 = 11.7 + 71 \times (0.7181 + 0.025)^2 = 50.906 \text{ kg} \times \text{m}^2,$$

$$I_{yy} = I_{yy}(CoG) + m_d \times Z_g^2 = 13 + 71 \times (0.7181 + 0.025)^2 = 52.206 \text{ kg} \times \text{m}^2.$$

The following table shows the moments of inertia referred to the scooter's ground reference system that will be used in the simulation (see Table 4).

Road Profiles

The profile followed by the road will be defined as a random road profile according to ISO 8608 [36]. Table 5 shows the initial values of the power spectral density of vertical displacement (referred to Φ in this research), according to reference values of spatial frequency, $n_0 = 0.1$ cycles/m and the angular spatial frequency, $\Omega_0 = 1$ rad/m. According to this standard, 8 kinds of road surface profile are established, varying from A to H (from lowest to highest degree of roughness).

Table 5 ISO 8608 values of $\Phi(n_0)$ and $\Phi(\Omega_0)$ [36]

Road class	$\Phi(n_0)(10^{-6}\text{m}^3)$		$\Phi(\Omega_0)(10^{-6}\text{m}^3)$	
	Lower limit	Upper limit	Lower limit	Upper limit
A	–	32	–	2
B	32	128	2	8
C	128	512	8	32
D	512	2048	32	128
E	2048	8192	128	512
F	8192	32,768	512	2048
G	32,768	131,072	2048	8192
H	131,072	–	8192	–
	$n_0 = 0.1$ cycles/m		$\Omega_0 = 1$ rad/m	

Table 6 ISO 8608 values of $\Phi(\Omega_0)$ selected

$\Phi(\Omega_0)$ value considered (10^{-6}m^3)	Road class limits		Class name	Rating
	Upper limit	Lower limit		
2	A	B	AB	Very good–good
8	B	C	BC	Good–regular
32	C	D	CD	Regular–poor
128	D	E	DE	Poor–very poor
512	E	F	EF	Very poor–fateful

The value of $\Phi(\Omega_0)$ will be considered as shown in Table 5. Five road classes to be studied have been defined, called AB, BC, CD, DE and EF. The first letter refers to the road class defined in Table 5 with that upper limit and, the second, refers to the letter of this table that has said lower limit, which coincide.

From these values, the ISO 8608 standard defines the

roughness of the road surface profile according to the following PSD equations for vertical displacement:

$$\Phi(n) = \Phi(n_0) \times \left(\frac{n}{n_0}\right)^{-2}, \tag{14}$$

$$\Phi(\Omega) = \Phi(\Omega_0) \times \left(\frac{\Omega}{\Omega_0}\right)^{-2}. \tag{15}$$

For practical implementation, random road profiles have been generated as a sum of sine functions as described by Tyan et al. [37]. This sum provides the elevation value of the road, $h(x)$, for each value of length traveled, s :

$$h(s) = \sum_{i=1}^{i=N} A_i \times \sin(\Omega_i \times s - \varphi_i), \tag{16}$$

where

- φ_i is the random phase angle that follows a uniform probabilistic distribution within the interval $[0, 2\pi)$.
- Ω_i is the angular spatial frequency i , which for N points will have a value of:

$$\Omega_i = \Omega_1 + \Delta\Omega \times (i - 1) [\text{rad/m}], \text{ con } \times \Delta\Omega = \frac{\Omega_N - \Omega_1}{N - 1} [\text{rad/s}]. \tag{17}$$

It has been selected next values $\Omega_1 = 0.02 \times \pi$ [rad/m] and $\Omega_N = 6 \times \pi$ [rad/m]. If A_i is the amplitude, it is defined according to the following equation:

$$A_i = \sqrt{\Phi(\Omega_i) \frac{\Delta\Omega}{\pi}}, i = 1, \dots, N. \tag{18}$$

In the previous equation, $\Phi(\Omega_i)$ [$m^2/(rad/m)$] are the values of the Power Spectral Density of displacement for the angular spatial frequency Ω_i . Now, Eq. (4) in its general form is

$$\Phi(\Omega_i) = \Phi(\Omega_0) \times \left(\frac{\Omega_i}{\Omega_0}\right)^{-w}. \tag{19}$$

The value $\Phi(\Omega_0)$ defines the PSD value for the reference wave value $\Omega_0 = 1$ rad/m. These values are defined for each road class in Table 6. The w value corresponds to the undulation value, the value of 2 being normally accepted for most road surfaces.

Realistically, e-scooter users will usually use roads in good condition. Thus, the first 5 road classes will be studied.

Table 7 Conventional comfort values of weighted r.m.s. acceleration

Comfort _{index}	Valuation
$< 0.315 \text{ m/s}^2$	No annoying
0.315 m/s^2 a 0.63 m/s^2	A little annoying
0.5 m/s^2 a 1 m/s^2	Something annoying
0.8 m/s^2 a 1.6 m/s^2	Annoying
1.25 m/s^2 a 2.5 m/s^2	Very annoying
$> 2 \text{ m/s}^2$	Extremely annoying

This will generate a total of 5 vertical road profiles that will be traveled at 5 constant velocities (5 km/h, 10 km/h, 15 km/h, 20 km/h and 25 km/h).

The following figure shows the 5 vertical profiles generated for each of the different road classes, depending on the length traveled, which has been set at 1 km.

If we zoom in the first 100 m, the calculated profiles can be better observed. It is shown also in Fig. 4.

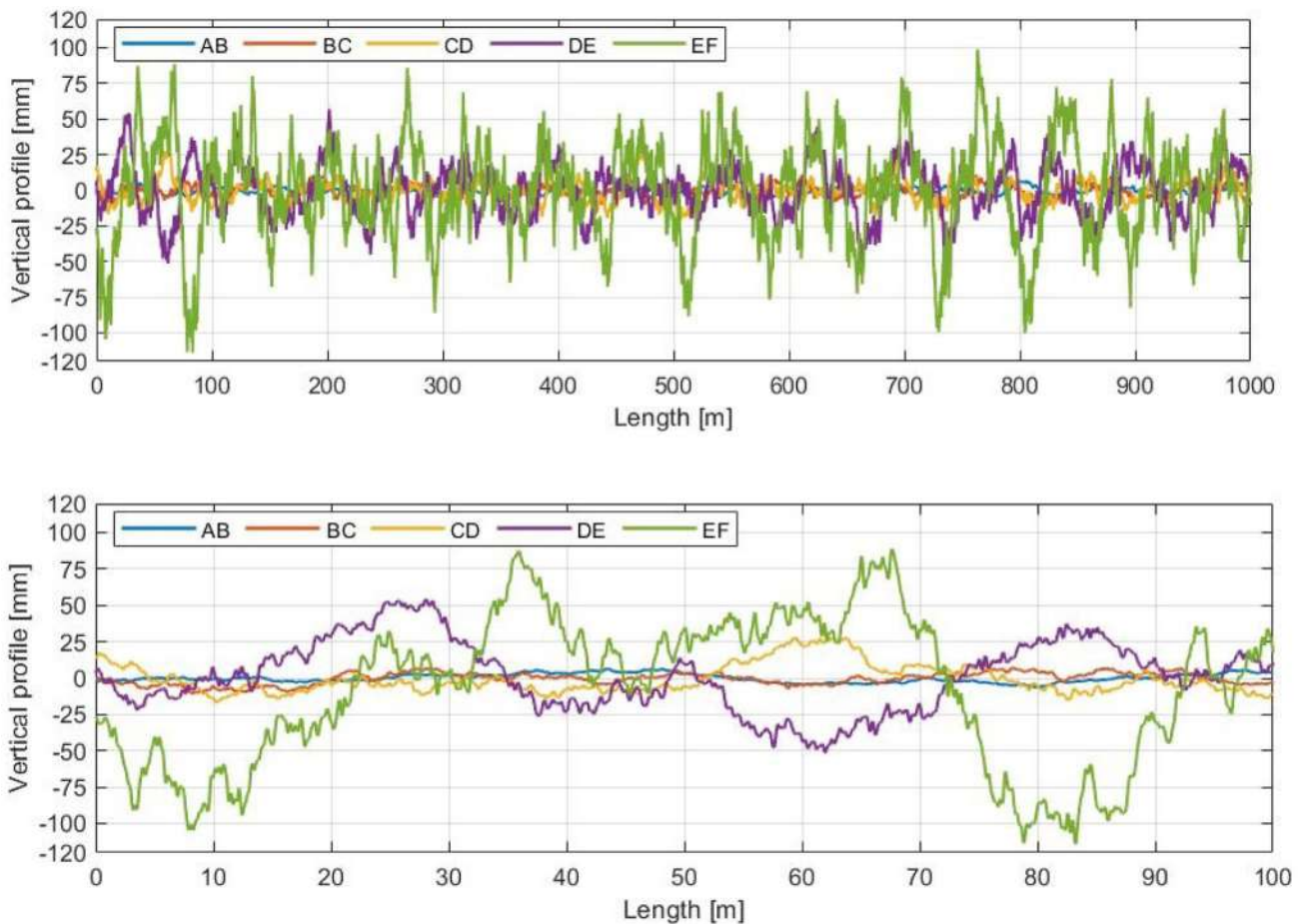


Fig. 4 Road profiles (1000 m and zoom for 100 m)

Comfort and Health Evaluation

For the evaluation of driver comfort of the simulated e-scooter model, the UNE2631 standard [38] will be applied according to the equations explained by Cano-Moreno et al. [27]. These equations allow the driver's comfort to be assessed against the vibrations received through the feet. For this, the accelerations of the dynamic simulation model have been sensed, in the vertical and longitudinal directions, the frequency filters indicated by the UNE2631 standard have been applied. The total vibration received will be called $\text{Comfort}_{\text{index}}$. This value thus defined will indicate the degree of driver comfort, with lower values of this index being more comfortable. It is formulated according to the following equation (see Table 7):

$$\text{Comfort}_{\text{index}} = [a_{wx}^2 + a_{wz}^2]^{\frac{1}{2}}. \quad (20)$$

Although the norm guides on the risks for the health only in activities that develop seated, health index is going to be studied as a guide. These vibrations have to be very similar to vibrations received by drivers of e-scooters which drive seated if the connection between e-scooter frame and seat is rigid. Health index can be expressed as:

$$\text{Health}_{\text{index}} = [1.6 \times a_{wx}^2 + a_{wz}^2]^{\frac{1}{2}}. \quad (21)$$

According to the research of Mathew et al. [17], in an analysis of more than 100 companies that rent e-scooters in Indianapolis (USA), they obtain that the most common trip has a route of 1.13 km and is 8 min long and the average velocity is 8.42 km/h. This means that to evaluate the effects of the vibrations received on the driver's health, it is necessary to observe the first area of the graph of the UNE2631 standard. In this area, the minimum range of values at 5 min of exposure to vibration has been considered. This range varies from 2 to 3 m/s^2 .

Design of Experiment and Data Analysis

To learn how vibrations affect to the e-scooter driver, dynamic simulations are carried out by varying four parameters: velocity, road condition, stiffness value of the wheel-road contact and stiffness value of the front suspension. To study its effects statistically, a complete factorial experiment design is proposed, with the following levels for each factor:

- Velocity [km/h], 5 values: 5, 10, 15, 20 and 25 km/h.

- Road condition, 5 roughness levels, according to the classes defined in Table 6: roads type AB, BC, CD, DE and EF
- Road-tire contact stiffness, k_w , of the two wheels of the e-scooter, 5 values [N/m]: 0.5E5, 1.E5, 2.E5, 3.E5 and 4.E5.
- Stiffness of the front suspension, k_{fs} , 3 values [N/m]: 1.3E5, 2.4E5 and 3.5E5 for flexible front suspension and 1.E6 for rigid suspension.

This means a total of 500 possible combinations, which have all been simulated to infer a comfort model and a health model for this type of e-scooter, driven on foot and have a front shock absorber. It should be noted that high stiffness values have not been included in the study because, increasingly, e-scooters have some type of front suspension system. In any case, the highest level of vibrations that would result from not wearing it has already been verified.

Compacted data provided from simulations of each case is going to be statistically modeled and analyzed. This work selected a standard linear multiple regression (LMR) method to relate the comfort index and health index to the velocity, roughness, Wheel stiffness and front suspension stiffness. A p value ≤ 0.05 will be considered significant. "Statgraphics Centurion 18" is the software tool used to perform this statistical analysis. These analyses will provide equations as shown in following equation:

$$y = a_0 + a_1 \times b_1 + a_2 \times b_2 + \dots + a_{n-1} \times b_{n-1} + a_n \times b_n, \quad (22)$$

where

- y is the response variable
- a_i are the regression coefficients, and
- b_i are the independent predictor variables.

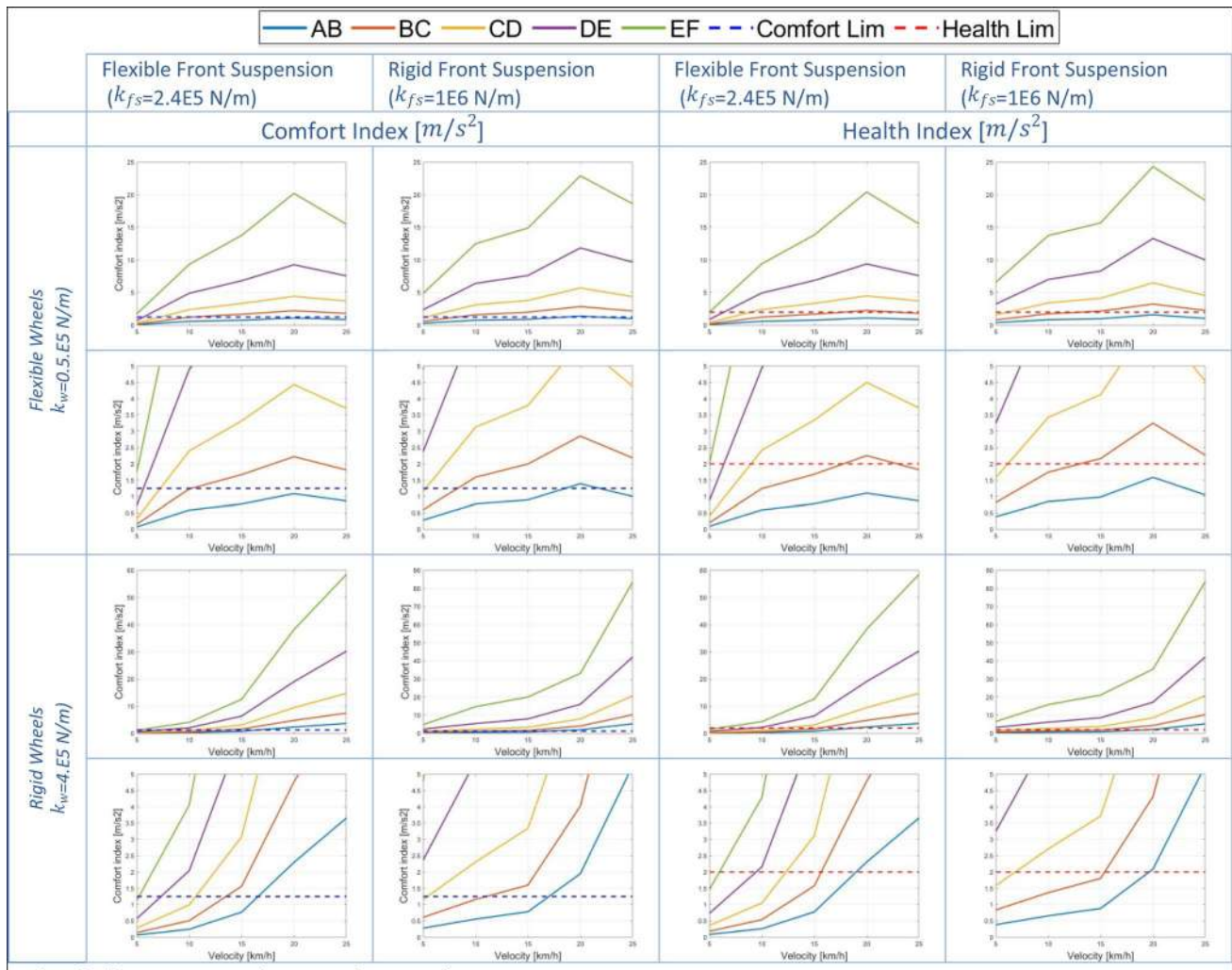
Results and Discussion

Table 8 shows the results obtained from similar 4 cases for the 5 velocities and 5 roughness or road condition values. Thus, a total of 100 results are shown, 25 per graph. The value of 1.25 m/s^2 for comfort (blue line) and health in 2 m/s^2 (red line) are established as a comfort limit and health limits, as limits from which there may be a minimum impact on the user's comfort and health, based on the recommendations of the standard UNE2631.

The following trends are observed:

If the road is in very good condition, type AB, comfort index evaluation following Table 7, for the worst point in each case:

Table 8 Results for rigid and flexible wheel–road contact and for rigid and flexible front suspension



	Front suspension		
	Soft	Hard	
Contact stiffness	Soft	Annoying	Very Annoying
	Hard	Extremely annoy- ing	Extremely annoying

Health limits are indicative, since the UNE2631 standard only uses them to assess the health of seated drivers. These limits are exceeded from a good road state, type AB, for the following cases:

Rigid wheel and soft front suspension, from 19 m/h.

Rigid wheel and hard front suspension, from 20 m/h.

For the same wheel and front spring, the better the less rigid.

The use of a soft front suspension system softens the level of vibrations received.

Table 9 Constants values for comfort and health index models

Parameter	Comfort		Health	
	Flexible	Rigid	Flexible	Rigid
Tire type				
A	5.76761	3.80702	5.36463	3.21599
B	2.04355	1.39177	1.92604	1.21529
C	0.511241	0.529007	0.509877	0.523539
D	17,261.7	19,440.9	17,936	19,554
E	23,265.6	0	31,871.4	0

When passing from one road state to the next worse, the comfort and health indexes doubles approximately, that is, the driver’s comfort decreases.

Health index is slightly higher than comfort index for the same layout.

Fig. 5 Statistical results: observed/predicted graph for “log (Comfort_{index})”, flexible tires (left) and rigid tires (right)

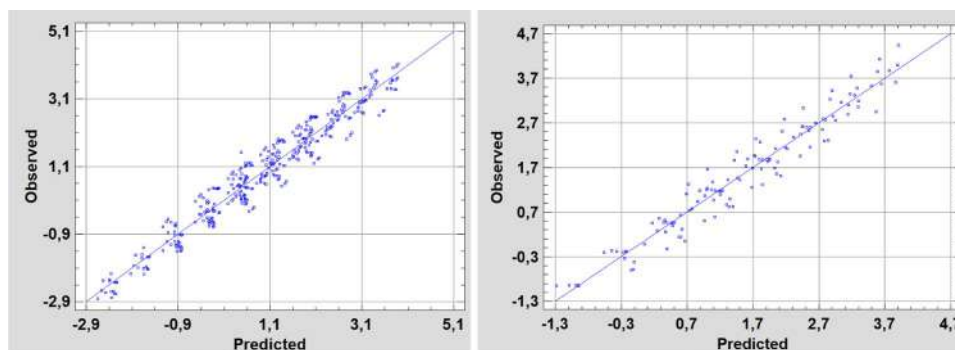


Table 10 Parameter values considered as extreme values

Front suspension	Extreme	Vel. [km/h]	Roughness level	$k_w \times 1.E5 [N/m]$	$k_{fs} \times 1.E5 [N/m]$
Rigid	Min	5	2	0.5	1.3
	Max	25	512	4	3.5
Flexible	Min	5	5	0.5	10
	Max	25	512	4	10

Statistical Models: Comfort, Health and Roughness

A multiple regression statistical analysis has been performed, relating the acceleration values associated with the comfort and health indexes with velocity (*V*), roughness level (*R*) and the stiffness values of the wheel and the front suspension. The 500 simulations have been divided for generating predictions for flexible tires and rigid tires. Thus, the first 375 simulations for road–tire contact stiffness, k_w , of 1.3E5, 2.4E5 and 3.5E5 N/m. The second models are based on 125 simulations for road–tire contact stiffness of 1.E6 N/m.

The following equation has been obtained with an adjusted R-square value of more than 94% for all comfort index and health index models. The dependent variables studied was log (Comfort_{index}) and log (Health_{index}), but the following equation shows the Comfort_{Index} and Health_{index}. Both indexes, for flexible and rigid tires, have the same equation with different constants defined in (see Table 9)

$$\text{Comfort}_{\text{index}} = e^{\left(-A+B \times \ln(V)+C \times n(R)-D \times \left(\frac{1}{k_w}\right)-E \times \left(\frac{1}{k_{fs}}\right)\right)} \quad (23)$$

Figure 5 shows the forecast of the model against the actual data. Health and Comfort models have a high similarity for the same cases, rigid and flexible suspension. Thus, linearity only of comfort indexes has been presented. These graphs show a high linearity for both models.

This developed statistical model shows the following trends:

- Decreased comfort of the driver with increased velocity, increasing the Comfort_{index}. This also occurs with

Table 11 Comfort factors extreme values

Case	Max/Min				Index values Min–Max [m/s ²]
	C_v	C_r	C_w	C_{fs}	
Comfort (flexible)	26.82	17.03	1.35	1.12	0.07–48.91
Comfort (rigid)	9.39	18.79	1.41	1.00	0.20–50.63
Health (flexible)	22.19	16.90	1.37	1.17	0.08–48.42
Health (rigid)	7.07	18.23	1.41	1.00	0.28–50.05

the increase in roughness and, therefore, with poor road conditions.

- Increasing both the stiffness of the wheels and the front suspension means that the terms $\frac{1}{k_w}$ and $\frac{1}{k_{fs}}$ remain less, which means that the Comfort_{index} increases and, therefore, reduces passenger comfort.

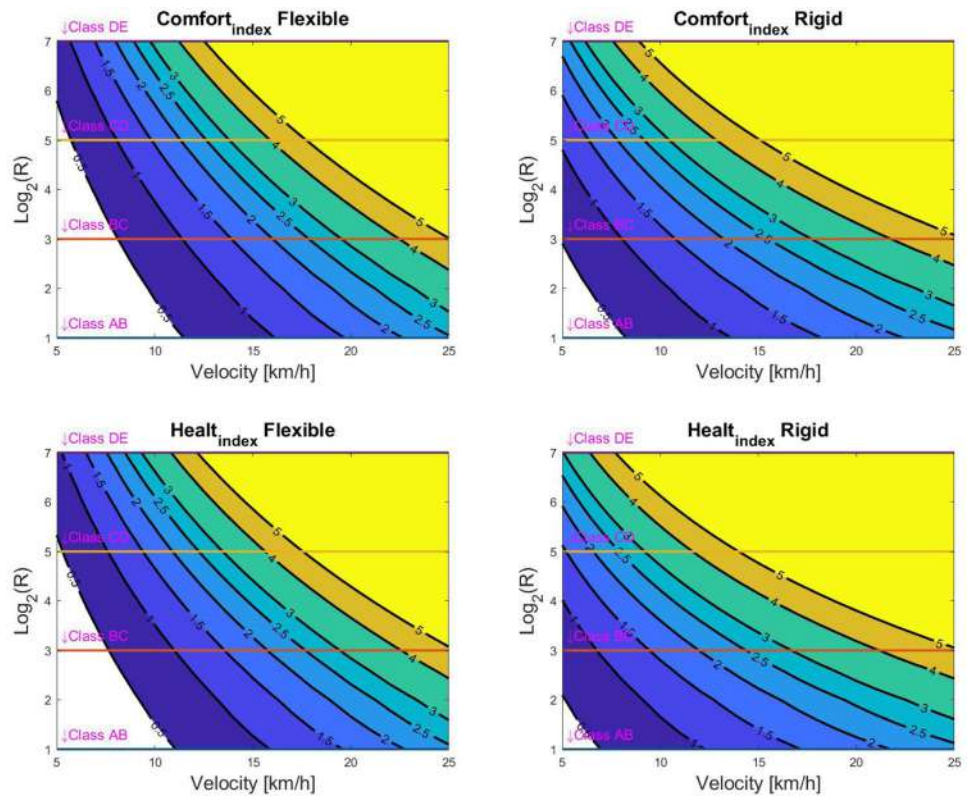
The general model described in Eq. (23) can be formulated as a model that explains the variation of both, comfort and health indexes, of an e-scooter driver as a multiplication of 4 independent factors associated with the velocity, roughness or condition of the road, wheel stiffness and stiffness of the front suspension. Each factor would have units of $\sqrt[4]{m/s^2}$. The following equation shows their relationship:

$$\frac{\text{Comfort}_{\text{index}}}{\text{Health}_{\text{index}}} = C_v \times C_R \times C_w \times C_{fs}, \quad (24)$$

where.

C_v is the velocity factor, defined in the following equation as:

Fig. 6 Comfort and Health contour maps for rigid and flexible front suspension models



$$C_v = e^{-A} \times e^{B \times \ln(v)}, \tag{25}$$

C_r is the roughness factor, which can be simplified according to:

$$C_r = e^{C \times \ln(R)} \cong e^{0.5 \times \ln(R)} \cong \sqrt{R}, \tag{26}$$

C_w is the road–wheel contact stiffness factor, which varies according to the following exponential equation:

$$C_w = e^{-D \left(\frac{1}{k_w} \right)}, \tag{27}$$

C_{fs} is the front stiffness factor, like the previous factor, C_w , it varies according to another exponential equation:

$$C_{fs} = e^{-E \left(\frac{1}{k_{fs}} \right)}. \tag{28}$$

To better understand the behavior of these models, extreme values for different parameters have been selected. This selection is shown in Table 10.

Table 11 shows how the factors defined in Eq. (24) vary for the extreme situations defined in Table 10.

Results show a similar variation in the range of comfort and health indices for the same type of front suspension. It is appreciated that the health index is higher than the comfort index in its minimum value (14% for flexible and 40% for rigid), and slightly higher in its maximum value.

Table 12 Velocities values [km/h] for constant comfort index of 1.5 m/s²

	AB	BC	CD	DE
Comfort (flexible)	20	14	10	7
Comfort (rigid)	18	11	6	<5

Table 13 Velocities values [km/h] for constant health index of 2 m/s²

	AB	BC	CD	DE
Health (flexible)	23	16	11	7.5
Health (rigid)	21	12	6	<5

A great asymmetry is observed in the contribution of each factor to the final value of each index. Thus, the speed factor, C_v , is much more decisive in the case of flexible front suspension. The factor associated with the front suspension, the least influential at present, is slightly higher for the health than comfort index. However, the roughness factors, C_r , and the wheel–road contact stiffness factor, C_w , are more influential in the case of rigid than flexible front suspension.

On the other hand, the mathematical expressions of comfort and health models (Eq. 24) can be drawn (see Fig. 6) as

roughness and velocity-dependent contour maps for a model with fixed stiffness values.

It has been selected as an example a contact stiffness value of $k_w = 1.E5$ N/m and for front suspension stiffness $k_{fs} = 2.4E5$ N/m (flexible layout) and $k_{fs} = 1E6$ N/m (rigid layout). These lines can be considered like maps of the comfort and health index. Since each line represents constant values of comfort and health, it can be calculated what velocity allows drivers to maintain a constant comfort value for different road roughness values.

For the same layout, there are differences between the health and comfort maps. In general, it is observed that for the same isoline value, they have lower velocity values (more conservative) for the health map than for the comfort one. This difference is less pronounced for high isoline values (see the 5 m/s^2 isoline).

For different layouts, it is observed that with a flexible suspension e-scooter higher speeds can be achieved for constant comfort values. Thus, if we consider the comfort index isoline of 1.5 m/s^2 , equivalent velocities for this level of driver comfort can be obtained. These velocities are summarized in Table 12 for flexible and rigid layout. In general, flexible layout allows reaching higher speed values than rigid layout. For rigid layout, the 1.5 m/s^2 isoline of its comfort map does not reach DE road class.

For health index maps, the tendency is similar. In this case, the 2 m/s^2 isoline has been selected. The equivalent speeds according to the road class have been included in Table 13.

A third statistical model has been achieved for relating Comfort and Health indexes directly. A simple linear regression model has been developed with an adjusted R-square of more than 99%. Next equation shows that health index is statistically higher than comfort index. As the following equations show, the main offset and slope appear for rigid front suspensions:

$$[\text{Flexible}] \text{Health}_{\text{index}} = 0.058466 + 1.0007 \times \text{Comfort}_{\text{index}} \quad (29)$$

$$[\text{Rigid}] \text{Health}_{\text{index}} = 0.3943021 + 1.01041 \times \text{Comfort}_{\text{index}} \quad (30)$$

On the other hand, from these comfort and health models a theoretical method could be inferred to measure the roughness of a road through the measured accelerations since, for a constant velocity and stiffness, the roughness can be obtained from Eq. (24), that can be written as follows:

$$f(\ddot{x}) = C_v \times C_R \times C_w \times C_{fs} \quad (31)$$

Being $f(\ddot{x})$, function dependent on the accelerations (e.g., comfort or health indexes) and, as $C_r = \sqrt{R}$, would have to be expressed as:

$$R = \left(\frac{C_v \times C_w \times C_{fs}}{f(\ddot{x})} \right)^2 = \left(\frac{\text{Constant}}{f(\ddot{x})} \right)^2 \quad (32)$$

Depending on the value of R , the state of the road could be obtained according to Table 5.

Conclusions and Future Remarks

In this paper, for the first time, the impact of vibrations received by e-scooter on drivers' comfort and health has been quantitatively evaluated. The study is based on Multibody dynamic simulations carried out on Simscape (Simulink-Matlab).

In summary, a Multibody model of e-scooter with front suspension, driven on foot, has been developed. With this model, 500 dynamic simulations have been carried out, under a factorial experiment design with 4 factors, 3 of them with 5 levels and one with 4. The factors are the state of the road (roughness), velocity, road–tire contact stiffness and the front suspension stiffness. With the acceleration results of these simulations, the comfort and health indexes have been obtained according to the UNE2631 standard. With these indices, four multiple regression models have been developed that explain the variability of these indices based on these 4 factors. There are two models for a flexible front suspension system and two for a rigid front suspension system. All models have the same formulation, but with different weights for the variables. These models, with an adjusted R squared value greater than 94%, allow evaluating the effects of the vibrations transmitted by an e-scooter to the driver's body. The models indicate that the influence of these 4 factors is independent and multiplicative.

Analyzing the results, it can be concluded that, for a given velocity, the state of the road is decisive for passenger comfort, improving with low stiffness values. These indices can always be improved by reducing velocity. This suggests the need to install an accelerometer at the base of the e-scooter, process these accelerations in accordance with UNE2631 and indicate in some way (RGB LED, for example) if these travel conditions are comfortable or/and healthy or not.

The low influence of the stiffness ranges used in the transmission of vibrations suggests that there is a large field of action in the design of future suspensions (including wheels) to further improve the factors associated with suspensions. The roughness of the road cannot be changed, and the velocity must be competitive to solve the problem of the last mile and thus continue to contribute to the brake of climate change. Thus, the study of comfort and safety should be a design requirement for future e-scooters.

The results show that for velocities of up to 25 km/h, the state of the road must be good enough not to produce vibrations that are not comfortable or harmful to health. For one of the best cases, with a medium stiffness value of a flexible suspension (2.4E5 N/m) and pneumatic tires (1.E5 N/m), speed limitations can be calculated from contour maps. On one hand, for a rough road type CD (regular-poor), a velocity of 8 km/h begins to be uncomfortable (isoline of 1 m/s²) and that 11 km/h could be harmful to health (isoline of 2 m/s²), for short trips. On the other hand, for a AB road (very good-good), velocities of 16 km/h and 23 km/h are the limits for comfort and health, for the same isolines analyzed previously.

Derived from the statistical models, a new way of measuring the roughness has been proposed and that will be one of the future works to adjust and validate it.

As an immediate future work, we intend to apply this methodology, initiated by Cano-Moreno et al. [9] and study the effect of vibrations on more designs of the new electric means of transport that are already on the market. It is also intended to introduce the study of the vibrations received through the hand, not only those of the whole body. Another future line will be oriented to study the natural frequencies of these mechanical systems, as well as their stability to also assess the safety of drivers.

References

1. Global EV Outlook 2019—Analysis <https://www.iea.org/reports/global-ev-outlook-2019>. Accessed 13 Dec 2019
2. Last mile (transportation) (2019) [https://en.wikipedia.org/w/index.php?title=Last_mile_\(transportation\)&oldid=929422005](https://en.wikipedia.org/w/index.php?title=Last_mile_(transportation)&oldid=929422005). Accessed 12 Dec 2019
3. Cossu P (2016) Clean last mile transport and logistics management for smart and efficient local governments in Europe. *Transport Res Proc* 14:1523–1532. <https://doi.org/10.1016/j.trpro.2016.05.117>
4. Using Bicycles for the First and Last Mile of a Commute September 2009, <http://transweb.sjsu.edu/research/using-bicycles-first-and-last-mile-commute-september-2009>. Accessed 12 Dec 2019
5. Convenience Is King, <https://www.good.is/articles/convenienc-e-is-king>. Accessed 12 Dec 2019
6. Zax D Can driverless pod cars solve the “Last-Mile Problem”?, <https://www.technologyreview.com/s/425055/can-driverless-pod-cars-solve-the-last-mile-problem/>. Accessed 12 Dec 2019
7. Yvkoff L Are motorized shoes the last-mile transport answer?, <https://www.cnet.com/roadshow/news/are-motorized-shoes-the-last-mile-transport-answer/>. Accessed 12 Dec 2019
8. Katzev R (2003) Car sharing: a new approach to urban transportation problems. *Anal Soc Issues Public Policy* 3:65–86. <https://doi.org/10.1111/j.1530-2415.2003.00015.x>
9. Efthymiou D, Antoniou C, Waddell P (2012) Factors affecting the adoption of vehicle sharing systems by young drivers. *Transp Policy*. <https://doi.org/10.1016/j.tranpol.2013.04.009>
10. Arena M, Azzone G, Bengo I (2017) Traditional and innovative vehicle-sharing models. In: *Research for Development*, pp 25–36 (2017)
11. Gössling S (2020) Integrating e-scooters in urban transportation: problems, policies, and the prospect of system change. *Transport Res Part D Transp Environ* 79:102230. <https://doi.org/10.1016/j.trd.2020.102230>
12. Europe Electric Scooters and Motorcycles Market Size | Two-Wheeler Industry Report | 2019–2025, <https://www.psmarketresearch.com/market-analysis/europe-electric-scooters-and-motorcycles-market>. Accessed 12 Dec 2019
13. Weinert J, Ma C, Cherry C (2007) The transition to electric bikes in China: history and key reasons for rapid growth. *Transportation* 34:301–318. <https://doi.org/10.1007/s11116-007-9118-8>
14. Weinert J, Ogden J, Sperling D, Burke A (2008) The future of electric two-wheelers and electric vehicles in China. *Energy Policy* 36:2544–2555. <https://doi.org/10.1016/j.enpol.2008.03.008>
15. Kopp P (2011) The unpredicted rise of motorcycles: a cost benefit analysis. *Transp Policy* 18:613–622. <https://doi.org/10.1016/j.tranpol.2011.03.002>
16. Hardt C, Bogenberger K (2017) Usability of escooters in urban environments—a pilot study. In: *2017 IEEE Intelligent Vehicles Symposium (IV)*, pp 1650–1657 (2017)
17. Mathew JK, Liu M, Seeder S, Li H, Bullock DM (2019) Analysis of E-scooter trips and their temporal usage patterns. *Institute of Transportation Engineers. ITE J Washington*. 89:44–49
18. Electric Scooter Reviews—Prices, Specs, Videos, Photos, <https://electricridereview.com/category/scooter/>. Accessed 13 Jun 2019
19. Hardt C, Bogenberger K (2019) Usage of e-scooters in urban environments. *Transp Res Proc* 37:155–162. <https://doi.org/10.1016/j.trpro.2018.12.178>
20. Ataei M, Asadi E, Goodarzi A, Khajepour A, Khamesee MB (2015) Multi-objective optimization of a hybrid electromagnetic suspension system for ride comfort, road holding and regenerated power. *J Vib Control*. <https://doi.org/10.1177/1077546315585219>
21. Cossalter V, Doria A, Garbin S, Lot R (2006) Frequency-domain method for evaluating the ride comfort of a motorcycle. *Veh Syst Dyn* 44:339–355. <https://doi.org/10.1080/00423110500420712>
22. Jiang X, Yan F, Chen W, Wang H (2018) Improving ride comfort of a heavy truck. In: *Presented at the (2018)*
23. Ripamonti F, Chiarabaglio A (2019) A smart solution for improving ride comfort in high-speed railway vehicles. *J Vib Control*. <https://doi.org/10.1177/1077546319843377>
24. Singh D (2019) Ride comfort analysis of passenger body dynamics in active quarter car model using adaptive neuro-fuzzy inference system based super twisting sliding mode control. *J Vib Control*. <https://doi.org/10.1177/1077546319840899>
25. Szydło K, Wolszczak P, Longwic R, Litak G, Dziubinski M, Drozd A (2020) Assessment of Lift passenger comfort by the Hilbert-Huang transform. *J Vib Eng Technol* 8:373–380. <https://doi.org/10.1007/s42417-019-00184-3>
26. Sharma R, Goyal K (2017) Improved suspension design of indian railway general sleeper ICF coach for optimum ride comfort. *J Vib Eng Technol* 5:547–556
27. Cano-Moreno JD, Islán M, Blaya F, D’Amato R, Juanes J, Soriano E (2019) Methodology for the study of the influence of e-scooter vibrations on human health and comfort. In: *Seventh International Conference on technological ecosystems for enhancing multicultural (TEEM’19)*, pp. 445–451. ACM (2019)
28. Agostinacchio M, Ciampa D, Olita S (2014) The vibrations induced by surface irregularities in road pavements—a Matlab® approach. *Eur Transp Res Rev* 6:267–275. <https://doi.org/10.1007/s12544-013-0127-8>
29. Ramji K, Goel VK, Saran VH (2002) Stiffness properties of small-sized pneumatic tyres. *Proc Inst Mech Eng Part D* 216:107–114. <https://doi.org/10.1243/0954407021528959>

30. Heißing B, Ersoy M (eds) (2011) Chassis Handbook: Fundamentals. Perspectives. Vieweg+Teubner Verlag, Driving Dynamics, Components, Mechatronics
31. Ferdek U, Luczko J (2016) Vibration analysis of a half-car model with semi-active damping. *J Theoret Appl Mech.* 54:321–332. <https://doi.org/10.15632/jtam-pl.54.2.321>
32. admin: Los nuevos patinetes de Wind llegan a Madrid » Patinete Madrid, <https://patinetemadrid.com/noticias/los-nuevos-patinetes-de-wind-llegan-a-madrid/>, (2019). Accessed 3 Dec 2019
33. Chandler R, Clauser C, McConville J, Reynolds H, Young J (1975) Investigation of inertial properties of the human body Technical Report (AMRL-TR-74-137). Wright-Patterson Air Force Base, OH
34. Santschi WR, DuBois J, Omoto C (1963) Moments of inertia and centers of gravity of the living human body. North American Aviation Inc, Los Angeles. Accessed 23 Oct 2019
35. Estatura media de hombres y mujeres en todo el mundo, <https://www.datosmundial.com/estatura-promedio.php>
36. ISO 8608:2016. Mechanical vibration—road surface profiles—Reporting of measured data
37. Tyan F, Hong Y-F, Shun R, Tu H, Jeng W (2009) Generation of random road profiles. *J Adv Eng* 4:1373–1378
38. Standar UNE-ISO 2631–1:2008. Mechanical vibration and shock. Evaluation of human exposure to whole-body vibration. Part 1: General requirements.

Publisher's Note Springer Nature remains neutral with regard to jurisdictional claims in published maps and institutional affiliations.